1431

Investigation of Methods for Global Gravity Field Recovery from the Dense ERS-1 Geodetic Mission Altimetry

O Ba Andersen and P Knudsen (Kort- og Matrikelstyrelsen, Copenhagen NV, Denmark. E-mail: oa@kms.min.dk and pk@kms.min.dk)
C C Tscherning (Geofysisk Dept., University of Copenhagen, Copenhagen Ø, Denmark, E-mail: cct@osiris.gfy.ku.dk)

Abstract. A number of different methods for gravity field prediction from altimetry were investigated in an area of the Greenland-Iceland-Norwegian sea. The investigation was carried out in an area with a relatively small oceanographic signal. The methods investigated were gravity field prediction using inverse Stokes method implemented using FFT and least squares collocation (LSC). The LSC procedure was investigated using different numbers of altimeter data and different procedures. These were gravity field prediction from direct altimetric observations and gravity field prediction using altimeter-derived along-track deflections of the vertical.

For the derivation of the global marine gravity field we decided to use inverse Stokes method implemented using FFT as it gives virtually the same result as would have been obtained using LSC directly. However we are missing the associated error-estimates which are obtained using LSC. These may, however, be estimated from the error-estimates obtained in the test area, by scaling the error-estimate using the ration between the local gravity variation and the value in the test area.

Introduction.

Since the completion of the geodetic phase of the ERS-1 satellite a global data set of high quality with a very homogeneous distribution has been available. In areas where good ship-gravity is available, we then have the possibility of testing gravity field prediction procedures as a function of the method and the data density used in the calculations. Such tests have earlier been carried out using satellite altimetry by, e.g. Rapp (1985, 1986). In Zhang & Blais (1995) results using Fast Fourier Transformation methods (FFT) and least-squares collocation (LSC) (Moritz, 1980) are compared, and it is concluded that the two methods give nearly identical results. Furthermore, several other approaches can be used. Rather than using direct height observations, there are also methods to use along track deflections of the vertical (DFV) or differences between the deflections, i.e.

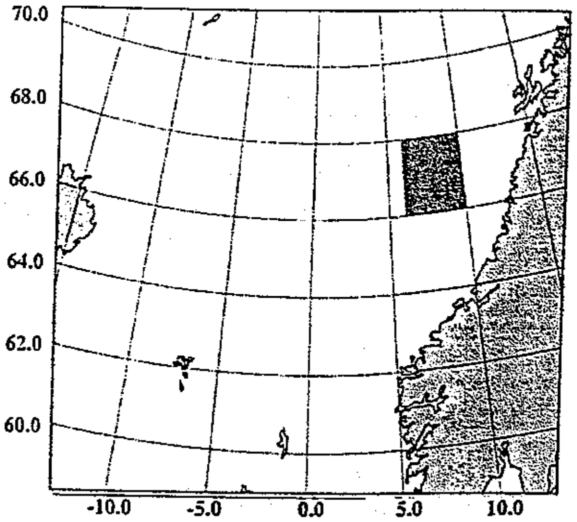

Figure 1. Area of investigation in the Greenland-Iceland-Norwegian (GIN) sea.

IAG Symp 116, 1996

gravity gradients (Rummel & Haagmans, 1990; Sandwell, 1984; Sandwell & Smith, 1992). These methods are mathematically closely related to methods which use sea-surface heights, which have been crossover adjusted using both bias and tilt parameters.

The selected area is located in the Greenland-Iceland-Norwegian Sea (GIN Sea) close to Norway as shown in Figure 1. This area was chosen as it had a very dense coverage of good marine gravimetric measurements. The test should preferably be conducted in an area with a small oceanographic signal, i.e. no currents and eddies. However, the test area did not fulfil this requirement (see Aas, 1994), as oceanographic data indicates, that the gravity signal due to non-stationary phenomena must be of the order of 2 - 3 mgal. The results obtained in this analysis indicate that this order of magnitude is correct. The modern marine gravimetric measurements are obtained from Amarok A/S (Norway), and the data set is supposed to have an error below 2 mgal. The location of these 816 marine measurements can be seen in Figure 3 and the derived free-air gravity field can be seen in Figure 4. Furthermore, statistics of the observed gravity field can be found in Table 1. Note, that the zero-level of the observed gravity field is somewhat uncertain.

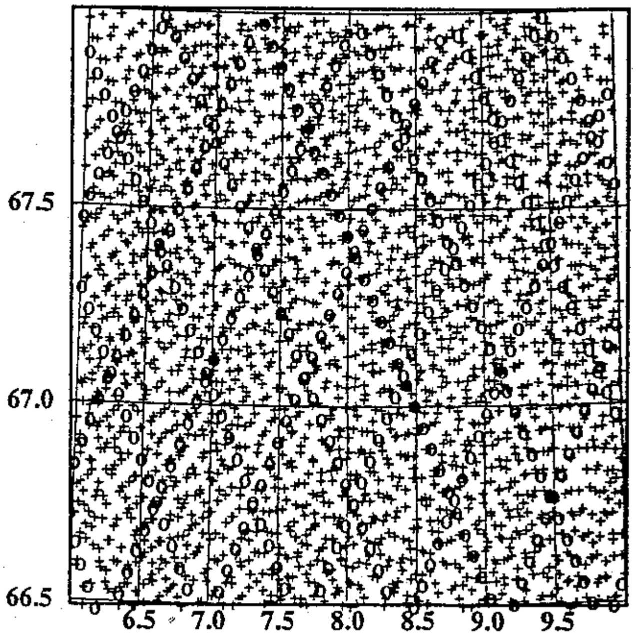

Figure 2 ERS-1 altimeter data from the 35-day mission (circles) and from the geodetic mission (crosses)

In this analysis we investigated several methods and data types. These are:

- inverse Stokes method implemented using FFT
- Least-squares collocation (LSC) using:
    (a) all altimeter data.
    (b) N altimeter data in each quadrant closest to the prediction point where N is 10, 15, 25, 30 and 40. (i.e. maximally 4*N points).
    (c) all altimeter-derived along-track deflections of the vertical (DFV)
    (d) the N altimeter-derived along-track DFV in each quadrant closest to the prediction point, where N is 10 and 25.
  - Furthermore a number of different data selection criteria were tested.

Table 1. Observed marine gravity field. Units are in mgal.

mean	std.dev	min	max.	error
3.3	17.2	-37.2	57.1	< 2.0

Gravity field prediction using least squares collocation (LSC).

Altimeter data were selected in the area bounded by 66°N and 68°N latitude and 6°E and 10°E longitude as shown in Figure 1. Stacked and cross-over adjusted ERS-1 data from the entire 35-day repeat cycle as well as ERS-1 data from the entire geodetic phase were used. The density and distribution of these data can be seen in Figure 2, where data from the 35-day repeat mission are shown as circles and data from the geodetic mission are shown with crosses.

OPR data from the 35-day repeat mission and Quick-look OPR data were used for the analysis. Initially the data were corrected for geophysical and environmental correction using the standard set of corrections. These include corrections for dry troposphere, wet troposphere, ionosphere, solid earth tide and elastic ocean tide correction, using the values provided in the Interim Geophysical Data Records containing the ERS-1 altimetry.

The error standard deviation associated with the stacked data was obtained from the standard deviation of the stacked observations divided by the square-root of the number of repeats used to compute the stacked observations (typically 18). This generally resulted in error standard deviations below 0.05m. 410 data from the 35 day cycle and 3333 data from the geodetic phase of the ERS-1 satellite were used. This gives a total of 3734 observations. Subsequently the contribution from the OSU91A spherical harmonic expansion complete to degree and order 360 (Rapp el al., 1991) was subtracted from the sea surface height observations. These residual height observations are shown in Figure 5

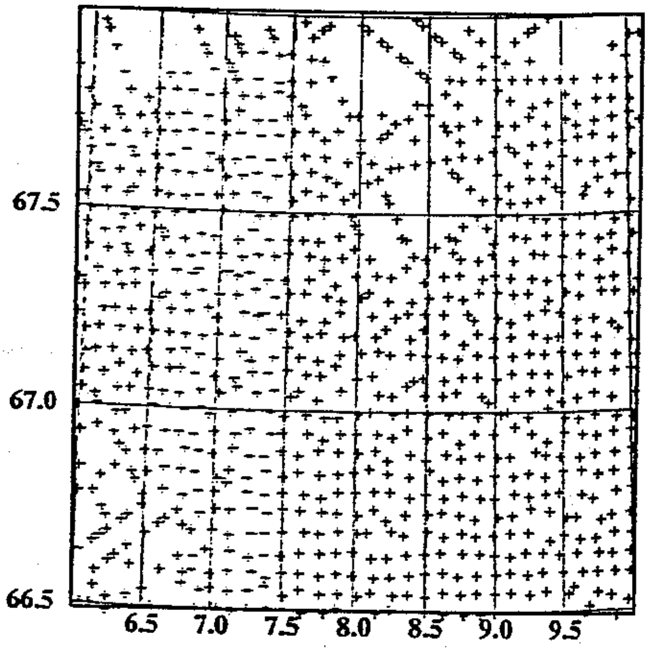

Figure 3 Location of marine gravity from Amarok A/S (Norway).

Since the data-distribution is very dense (Figure 2), observations were selected in cells having a size of 0.075° in latitude and 0.15° in longitude. The selection was done such that the observations with the smallest associated error estimate was selected. This selected data set consisted of 755 observations.

The observations were also used to calculate along-track deflections of the vertical. The along-track deflections of the vertical were calculated by simply taking the difference between consecutive points divided by the distance. This resulted in very noisy observations, where the observations with deviations larger than 10" or with a standard deviation larger than 4" were rejected as outliers. The resulting 2430 observations had a standard deviation of 2.9".

Empirical auto and cross-covariances were computed from the altimeter height observations relatively to the OSU91A geoid as well as from the marine gravity data using the program EMPCOV. The EMPCOV program computes such empirical covariance and cross-covarians functions from the observed data and is a part of the GRAVSOFT-program package (Tscherning et al. 1992, 1994). Similarly, a covariance function was computed using the stacked 35 day repeat data. As expected the stacked data has a slightly smaller variance than the original data (0.28 m^2 instead of 0.30 m^2).

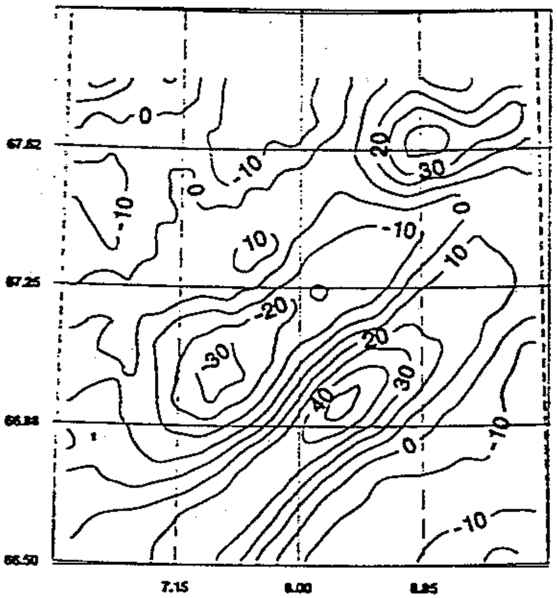

Figure 4 Free air gravity anomalies. OSU91A contribution removed. Units are in mgal.

The covariance function of the observed marine gravity data was fitted by an analytic expression using the COVFIT program (Knudsen, 1987, 1988). COVFIT is also part of the GRAVSOFT-program package and fits the empirical covariance function using an analytic base model by Tscherning & Rapp, (1974) like

$$K(P,Q) = \sum_{i=0}^{N} \epsilon_i(T,T) \left(\frac{R^2}{rr'} \right)^{i-1} P_i(\cos\psi) + \sum_{N-1}^{\infty} \sigma_i(T,T) \left(\frac{R_B^2}{rr'} \right)^{i+1} P_i(\cos\psi)$$

where ϵ_i(T,T) are the error degree-variances associated with the OSU91A, R is the mean earth radius, R_B is the radius of a Bjerhammar sphere (R_B<R), r and r' are the radial distances of P and Q respectively,ψ is the spherical distance between P and Q, σ_i are the so-called degree-variances, σ_i(T,T) = A/((i-1)(i-2)(i+4)), and A is a constant (= 4.0) in units of $(m/s)^2$.

From COVFIT the depth to the Bjerhammer sphere R-R_B is estimated to 7.3 km and the error degree variances factor of the OSU91A field to 0.375. The total gravity variance is 173.0 $mgal^2$. The empirical and the fitted analytic covariance functions can be found in Table 2.

Table 2. Empirical and analytically computed covariances. The covariances are shown as a function of spherical distance psi.

Sph. dist. (deg)	Geoid and geoid (m^2)		Geoid and gravity (m*mgal)		Gravity and gravity ($mgal^2$)		Geoid and DFV[1] (m*arcsec)	Gravity and DFV[a] (mgal*arcsec)	DFV and DFV[a] ($arcsec^2$)
Ψ	Emp.	Anal[b].	Emp.	Anal[b].	Emp.	Anal[b].	Anal[b].	Anal[b].	Anal[b].
0.00	0.095	0.109	3.004	3.106	167.6	173.0	0.000	0.00	3.85
0.05	0.083	0.107	3.160	2.996	157.7	161.1	0.100	-7.94	3.46
0.10	0.078	0.104	2.862	2.701	141.0	132.0	0.181	-13.41	2.52
0.15	0.070	0.098	2.356	2.300	99.1	97.2	0.235	-15.81	1.44
0.20	0.058	0.091	1.729	1.869	66.2	64.6	0.260	-15.84	0.48
0.25	0.047	0.084	1.239	1.460	33.5	37.6	0.263	-14.36	-0.25
0.30	0.036	0.077	0.765	1.102	8.5	17.1	0.249	-12.09	0.75
0.35	0.026	0.071	0.403	0.811	-4.9	2.7	0.224	-9.51	-1.04
0.40	0.018	0.065	0.206	0.589	-11.6	-6.2	0.194	-6.98	-1.16
0.45	0.011	0.060	0.108	0.432	-11.4	-10.9	0.162	-4.69	-1.14
0.50	0.008	0.056	0.130	0.332	-5.2	-12.3	0.133	-2.78	-1.03
0.55	0.003	0.053	0.075	0.278	-2.2	-11.3	0.107	-1.30	-0.85
0.60	-0.000	0.050	0.098	0.258	8.6	-8.8	0.087	-0.25	-0.65
0.65	-0.003	0.048	0.101	0.260	8.4	-5.5	0.072	0.38	-0.44
0.70	-0.008	0.046	0.052	0.275	11.4	-2.1	0.062	0.66	-0.25

[a] DFV is deflection of vertical.

[b] The analytically computed values are based on a fitting of the gravity covariance function.

Subsequently, the covariance function of the stacked altimeter data from the 35-day repeat mission was fitted using the procedure above. The result was a derived gravity variance of 357 $mgal^2$, a depth to the Bjerhammar sphere of 5.7 km and a weight factor for the error degree variances of 0.15. This covariance function was also used in the experiments, but it gave results than obtained using the covariance function obtained from the gravity data (Table 3).

The prediction using all altimeter data or along-track deflections were

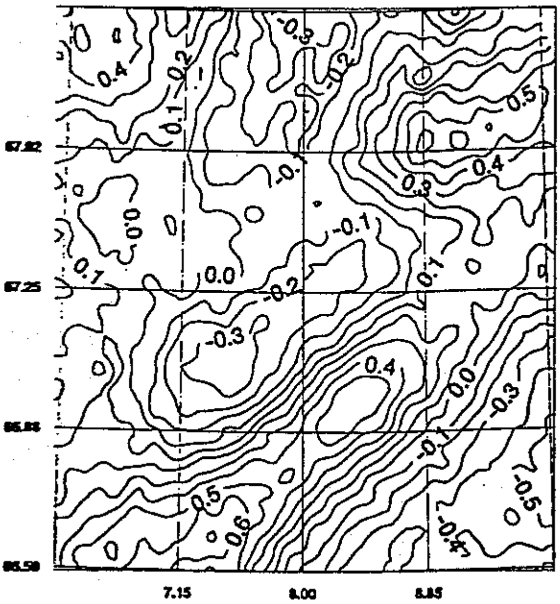

Figure 5 ERS-1 altimeter heights relative to the OSU91A geoid. Units are in meters.

done using the GEOCOL program. Results (i.e. differences between observed and calculated values) using collocation with all data are shown in Figure 6 The local predictions using up to N observations in each quadrant were done using the grid interpolation program GEOGRID.

One of the advantages of using LSC over FFT methods is the fact that LSC provides error-estimates. These error estimates can be seen in Figure 7.

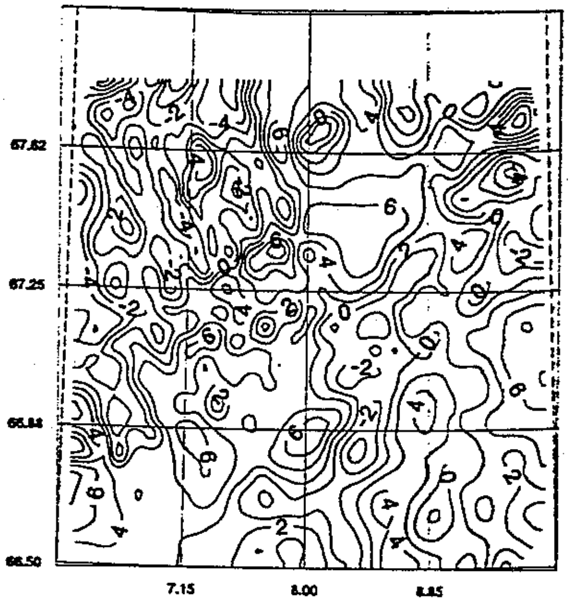

Figure 6 Gravity field residuals from ERS-1 data (observed minus predicted gravity). All height observations were used. Units are in mgal.

Gravity field prediction using inverse Stokes method implemented using FFT.

For this task the Quick Look OPR data from the ERS-1 Geodetic Mission were used. Prior to use the data were edited for gross errors and outliers. As editing criteria, conditions about the height and its standard deviation were used. The height relative to the OSU91A geoid model complete to degree and order 360 (Rapp et al., 1991) should be smaller than 20 m, and the standard deviation should be lower than 0.2 m relative to the trend through the data. This resulted in about 16 million altimeter data with global coverage (±82°latitude).

The mapping of the gravity field was carried out relative to the OSU91A geoid complete to degree and order 360 in 2° latitude by 10° longitude cells using GRAVSOFT software. Data were selected in an area that extends outside the 2° latitude by 10° longitude cells, namely in an area of 3° latitude by 12° longitude for the subsequent crossover analysis. In order to reduce effects of orbit errors, sea surface topography and sea level variability a bias and tilt were removed from each individual track. Subsequently, a crossover adjustment was carried out using bias, tilt, and quadratic terms. Then the sea surface heights were gridded in order to facilitate the use of FFT techniques for the conversion into gravity anomalies.

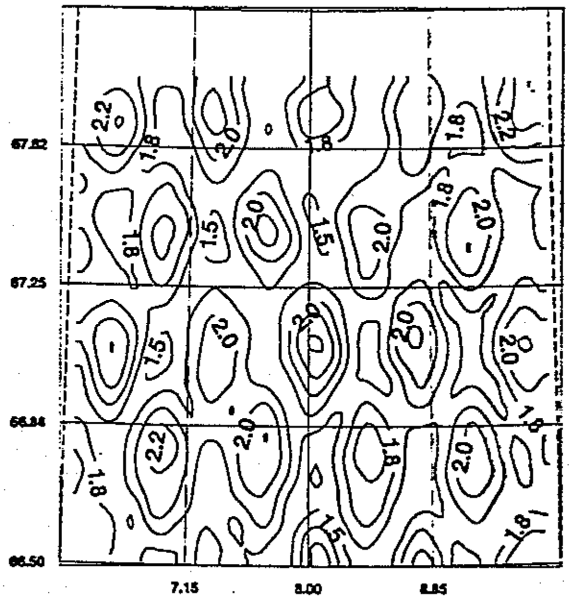

Figure 7 Gravity error estimate from prediction using all ERS-1 data. Units are in mgal.

Table 3. Results of gravity calculations expressed in terms of observed marine gravity minus predicted gravity. All units are in mgal. 816 observations were used for the comparison[a].

Met-hod	Data types	Nb.of data (N)	Difference				Error estimate		
			mean	std.	min	max.	mean	min	max
FFT	Heights		0.9	4.4	-13.5	16.7			
Collocation	Along track deflection of vertical (DFV)	all	2.0	4.0	-9.9	14.6	2.9	2.0	4.0
		10	-2.0	6.9	-24.3	18.7	6.9	5.7	8.9
		25	-1.8	5.1	-16.6	13.1	4.8	4.2	5.5
	Heights	all	1.6	4.2	-11.5	14.6	1.8	1.1	2.8
		10	1.4	8.1	-22.6	25.9	6.0	4.2	8.1
		15	1.2	6.5	-17.6	22.2	4.5	3.3	6.2
		25	1.3	5.2	-13.7	21.7	3.1	2.6	3.9
		40	1.3	4.7	-12.2	15.0	2.6	2.2	3.2
	Heights with best value per cell selected	15	1.3	4.7	-13.6	14.5	2.8	2.1	3.7
		25	1.4	4.6	-13.8	13.5	2.6	1.8	3.7
		40	1.4	4.5	-14.0	15.1	25	1.6	3.6
	Heights with one value per cell selected	25	1.8	4.8	-13.0	16.7	3.3	2.0	4.4
	Heights without accounting for individual data errors.	25	2.0	5.9	-18.9	17.5	2.4	2.2	2.4
	Heights using the covariance function derived from stacked altimtric data.	25	1.0	8.5	-26.4	24.7	2.9	2.6	3.0

[a] Area bounded by 66.5°N and 68.0°N latitude and 6.25°E and 9.75°E ^{2} longitude.

The gridding was performed using LSC with 18 points in each quadrant. Here an along track error covariance function was introduced in order to filter out remaining parts of the sea surface variability. The covariance function associated with the sea surface heights were fixed at a variance of $(0.3\ \text{m})^2$ and the correlation length at 15 km. The error covariance function was fixed at a variance of $(0.1\ \text{m})^2$ and the correlation length at 100 km along track. The noise variance was fixed at $(0.1\ \text{m})^2$. In order to reduce the effect of tapering in the FFT conversion the grids were extended to the dimension of 4° by 16° with a spacing of 1/16° in each direction.

The gravity field was derived from the height anomalies using FFT techniques (Forsberg and Solheim, 1988). In the frequency domain a weak noise filtering was applied at wavelengths shorter than 15 km. Finally, the OSU91A gravity field complete to degree and order 360 was restored, in order to obtain the free air gravity anomalies. The global free air gravity field in the area of investigation is shown in Figure 8.

Results and discussion.

The results of the gravity field predictions using different methods and different number of observations are summarized in Table 3.

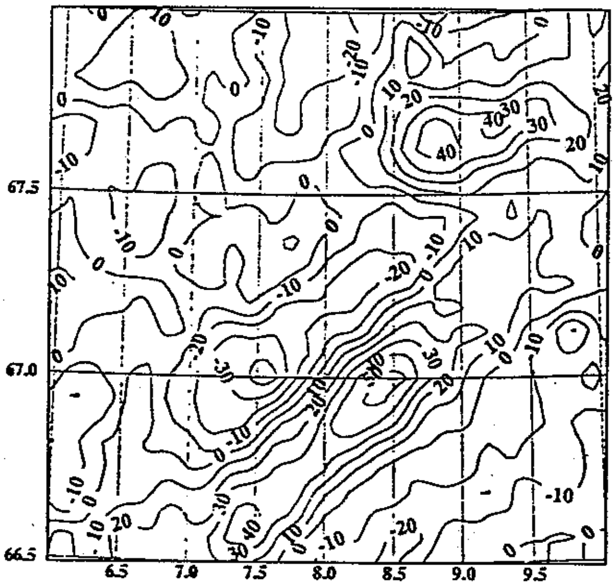

Figure 8 ERS-1 free air gravity anomalies derived using FFT. OSU91A contribution is subtracted. Units are in mgal. OSU91A

We see that the along track deflection of the vertical (DFV), despite the fewer data, gives the best results. However, if we want to compete with FFT, we must use N=25. This corresponds to maximally 4*25=100 data points, which because of the un-even distribution in practice amounted to 80 data points.

A few important results must be noted. These are, that the result is better if individual error estimates are used with the data, and that the result is better, if the observations with least error are selected in small cells. However, we can avoid the FFT-conversion to gravity anomalies. The local LSC method directly gives estimates of both the gravity anomaly and its error. The LSC procedure furthermore enables the simultaneous use of coastal as well as marine data.

For the actual production of a global gravity map for altimetry there is also other important criteria for the selection of the method. While the prediction of gravity is sensitive to the covariance function model used, then the gridding of the height data - which is a simple interpolation - is less sensitive. Furthermore, the determination of the covariance function used - which might be different from area to area - is a tedious task. Despite the availability of programs like COVFIT, the determination requires an experienced operator for its use.

We therefore decided to use the technique nearly identical to the one used in Andersen & Knudsen, (1995). This method gives virtually the same result as would have been obtained using LSC directly. However, we are missing the associated error-estimates. These may, however, be estimated from the error-estimated obtained in the test area, by scaling the error-estimate using the ration between the local gravity variation and the value in the test area.

Acknowledgement. This analysis is supported by the Danish Space Board. Thanks to ESA for putting the ERS-1 satellite into the geodetic mission and to D-PAF for preparing the OPR data.

References.

Aas, E.: De Norske Farvann. Institutt for Geofysikk, Oslo, 1994.

Andersen O. B. and P. Knudsen: Global altimetric gravity map from the ERS-1 geodetic mission (cycle 1). Earth Obs. Quarterly, 47, 1-5, 1995.

Forsberg, R., and D. Solheim: Performance of FFT methods in local gravity field modelling. Proc. Chapman Conference on Progress in the Determination of the Earths Gravity Field, Am. Geophys. Union, 100-103, 1988.

Knudsen, P.: Estimation and Modelling of the Local Empirical Covariance Function using gravity and satellite altimeter data. Bull. Geodesique, 61, 145-160, 1987.

Knudsen, P.: Determination of local empirical covariance functions from residual terrain reduced altimeter data. Reports of the Dep. of Geodetic Science and Surveying no. 395, The Ohio State University, Columbus, 1989.

Knudsen, P.: Integration of Altimetry and Gravimetry by Optimal Estimation Techniques. In Altimetry in Geodesy and Oceanography, edited by R.Rummel & F.Sanso, Lecture Notes in Earth Sci., 50, Springer Verlag, 453-466, 1993.

Knudsen, P., O.Ba. Andersen and C.C. Tscherning: Altimetric gravity anomalies in the Norwegian-Greenland Sea - Preliminary Results from the ERS-1 35 days repeat mission. Geophys. Res. Lett., 19(17), 1795-1798, 1992.

Moritz, H.: Advanced Physical Geodesy. H.Wichmann Verlag, Karlsruhe, 1980.

Rapp, R.H.: Detailled Gravity Anomalies and Sea Surface Heights derived from GEOS-3/SEASAT Altimeter Data. Rep. of the Dep. of Geod. Sci. and Surveying, No. 365, The Ohio State Univ., Columbus, 1985.

Rapp, R.H.: Gravity anomalies and sea surface heights derived from a combined Geos-3/SEASAT altimeter data set. J.Geoph.Res.,. 91, 4867-4876, 1986.

Rapp, R.H., Y.M. Wang and N.K. Pavlis: The Ohio State 1991 Geopotential and Sea Surface Topography Harmonic Coefficient Models. Rep. of the Dep. of . Science and Surv. 410, Ohio State Univ., Columbus, 1991.

Rummel, R. & R.H.N. Haagmans: Gravity gradients from satellite altimetry. Mar. Geodesy, 14, 1-12, 1990.

Sandwell, D. T.: A Detailed View of the South Pacific Geoid From Satellite Altimetry. J. Geophys. Res., 89, 1089-1105, 1984.

Sandwell, D.T. & W.H. Smith: Global Marine Gravity Field From ERS-1, Geosat and Seasat. Scripps Institute of Oceanography, La Jolla, CA, 1992.

Tscherning, C.C., P. Knudsen and R. Forsberg: Description of the GRAVSOFT package. Geophysical Institute, University of Copenhagen, Technical Report, 1991, 2nd. Ed. 1992, 3. Ed. 1993, 4. ed, 1994.

Tscherning, C.C., R. Forsberg and P. Knudsen: The GRAVSOFT package for geoid determination. Proc. First Continental Workshop on the Geoid in Europe, Prague, 327-334, Prague, 1992.

Tscherning, C.C. and R.H. Rapp: Closed Covariance Expressions for Gravity Anomalies, Geoid Undulations, and Deflections of the Vertical Implied by Anomaly Degree Variances. Rep208, Dept. of Geod. Sci. Surv., The Ohio State Univ., Columbus, 1974.

Zhang, C, & J.A.R. Blais: Comparison of methods for marine gravity determination from satellite altimetry data in the Labrador Sea. Bulletin Geodesique, 69(3), 173-180, 1995.